The Effect of Micro-Alloying of Sn Plating on Mitigation of Sn Whisker Growth

ALEKSANDRA DIMITROVSKA[1] and RADOVAN KOVACEVIC[1,2]

1.—School of Engineering, Research Center for Advanced Manufacturing, Southern Methodist University, Dallas, TX, USA. 2.—e-mail: kovacevi@lyle.smu.edu

Tin (Sn) is a key industrial material in coatings on various components in the electronics industry. However, Sn is prone to the development of filament-like whiskers, which is the leading cause of many types of damage to electronics reported in the last several decades. Due to its properties, a tin-lead (Sn-Pb) alloy coating can mitigate Sn whisker growth. However, the demand for Pb-free surface finishes has rekindled interest in the Sn whisker phenomenon. In order to achieve properties similar to those naturally developed in a Sn-Pb alloy coating, we carried out a study on deposited films with other Sn alloys, such as tin-bismuth (Sn-Bi), tin-zinc (Sn-Zn), and tin-copper (Sn-Cu), electrodeposited onto a brass substrate by utilizing a pulse plating technique. The results indicated that the Sn alloy films modified the columnar grain structure of pure Sn into an equiaxed grain structure and increased the incubation period of Sn whisker growth. The primary conclusions were based on analysis of the topography and microstructural characteristics in each case, as well as the stress distribution in the plated films computed by x-ray diffraction, and the amount of Sn whisker growth in each case, over 6 months under various environmental influences.

Key words: Sn whisker, XRD stress analysis, micro-alloying of Sn, Sn plating, Pb-free, equiaxed grain structure

INTRODUCTION

Tin (Sn), due to its great solderability, conductivity, low melting point, and good corrosion resistance, is employed as a protective coating for various electronic components.[1] However, the growth of whiskers from Sn plated finishes is a very common defect that affects the lifespan of many electronic components. There have been several studies done on this topic. Some of the primary behaviors that enhance whisker-like development of Sn include compressive stresses in the Sn plated coating and microstructural properties of the deposited Sn film.[2]

Alloying of Sn with lead (Pb), first discovered in the 1960s, has a retarding effect on Sn whisker growth.[3] The addition of Pb to Sn coating initiates modification of the columnar grain structure of pure Sn into an equiaxed grain structure; the same effect is believed to prevent localized surface disturbance in the deposit due to diffusion of elements.[1–3] With the legislation imposed by Europe and Asia on July 1, 2006, Pb, due to its toxic nature, is no longer permitted for use in electronic devices.[1,2] Since this legislation, there has not yet been a universally accepted, functionally equivalent replacement for the restricted Sn-Pb alloy coating, and failures of electronic equipment continue to be reported.[2]

Literature reports the effectiveness of plating by a pulsed current that can produce a deposited coating with significantly improved properties that cannot be achieved by plating with a continuous current.[4,5] Similarly, a report from Sandnes et al.[6] concluded that deposition of a tin-bismuth (Sn-Bi) alloy by the pulsed plating method, with concentrations as low as 3% Bi in the Sn film, could modify the columnar grain structure of Sn; the report stated that this

technique could mitigate Sn whisker growth. Another factor that allows Bi to form an equiaxed grain structure with Sn by the pulse plating method is the difference of 0.45 V between the potential coefficients of Bi and Sn, with Bi being more positive than Sn.[6] However, while the report from Sandnes et al. presented a detailed analysis on the modified microstructure of Sn, it provided no results on Sn whisker growth. In this study, in addition to the case with Sn-Bi alloy coating, we examined two other cases, tin-copper (Sn-Cu) and tin-zinc (Sn-Zn) alloy coatings, and their effect on Sn whisker growth.

Since Bi behaves like Pb when alloyed with Sn by the pulse plating technique, we selected elements with potential coefficients very close to that of Bi, and with similar potential difference with Sn as between Sn and Bi. The close candidate was Cu, with a potential coefficient of 0.34 V, approximately 0.47 V more positive than Sn. As expected after extensive experimentation, the Sn-Cu alloy coating did result in an equiaxed grain structure.[7] In addition, Zn forms a eutectic alloy with Sn. While this behavior of Sn-Zn resembled that of Sn-Bi and Sn-Pb alloys, Zn was not the best candidate because its potential coefficient is more negative than that of Sn by 0.63 V.[7]

However, for reference, we also selected Zn as a third case in this study. The three cases with alloy coatings were also compared with the case of a pure Sn coating in this study. Characteristics of the microstructure, the amount of Cu_6Sn_5 intermetallic compound (IMC) formed, and the stress distribution developed within a period of 6 months under different environmental influences were analyzed for each case. Experimental results revealed that the Sn-Bi, Sn-Cu, and Sn-Zn alloy coatings developed an equiaxed grain structure in the plated film, and the incubation period of Sn whisker growth compared with the pure Sn coating was significantly increased.

EXPERIMENTAL PROCEDURES

Flat rectangular-shaped Copper Development Association nomenclature 360 brass samples with dimensions of 5 cm × 2.54 cm × 0.1 cm and an area of approximately 13 cm[2] were used as substrates. In order to test the growth of Sn whiskers accurately, brass was selected as the substrate in each case. The coupons were cut by an abrasive water-jet machine, wet polished with #1000 silicon carbide (SiC) paper, wet polished with sodium bicarbonate to remove any residual grit, and rinsed with distilled water. They were then thermally destressed in a furnace at 200°C to 300°C for 1 h and finally treated with 10% concentrated sulfuric acid prior to plating. Each coupon was taped on the back with clear tape so that the plating was uniformly applied on only one side.

The electroplating station was equipped with a high-power supply (HP 6235) connected in series to a digital volt-ohm meter in order to measure the applied cell current precisely. A light motor with an attached impeller was used to provide agitation in the bath during plating. The plating bath used in this study for each experiment was matte Sn-based with a content of 150 mL commercial methylsulfonic acid (MSA) [75 mL MSA Technic + 75 mL water (H_2O)] operated at room temperature, and a Sn anode of 99.9% metal purity. The composition of each film and the plating conditions for each case are listed in Table I. In order to achieve an equiaxed microstructure, some parameters, such as plating current, duration of the pulse plating cycle, and the concentration of the alloying element in the Sn bath, were altered. In this study, after extensive experimentation, only the plating parameters that produced an equiaxed microstructure of the Sn alloyed film are presented for each case.

The layer thickness deposited, based on Faraday's equation, was controlled by the plating time and the current density applied during each alloy deposition.[8] Following the plating procedure, each sample was post-treated in a bath of water and neutralized in potassium hydroxide (KOH). Each plated sample was dried with an air fan and placed into the environmental chamber for a total aging period of 6 months following these steps: (1) the samples were stored in a clean plastic container at room temperature, (2) the samples were heated to a temperature of 60°C, and (3) the samples were

Table I. Composition and Plating Conditions for Each Case of Tin-Alloy Films

Tin-Alloy Composition	Original Compound of the Alloying Element	Composition of the Films	On Cycle (s)	Off Cycle (s)	Total Plating Time (min)	Plating Thickness (μm)	Current (A)
Pure Sn	MSA Sn bath	100%Sn (Pure Sn bath)	N/A	N/A	5	3	0.6
Sn-Bi	$Bi(NO_3)_3 \times 5H_2O$	80%Sn-20%Bi (Sn bath doped with 40 mmol Bi)	30	120	5	3	0.2
Sn-Cu	$CuCl_2 \times 2H_2O$	80%Sn-20%Cu (Sn bath doped with 40 mmol Cu)	30	5	5	3	0.6
Sn-Zn	$ZnSO_4 \times 7H_2O$	80%Sn-20%Zn (Sn bath doped with 40 mmol Zn)	30	120	5	3	0.6

exposed to 95% humidity in an environmental chamber.

All samples were carefully inspected over the entire surface area of 13 cm². However, the samples were cut, measured, and analyzed at their centers (taken as average data) over a measured area of 20 μm × 20 μm from the total surface of each sample. The time interval for inspection of each sample was every 2 weeks, up to a total time period of 6 months. The surfaces of the electroplated samples were analyzed and inspected for whisker growth using a scanning electron microscope (SEM), operated at 5 kV and 30 pA, and the cross-sections were prepared using a dual-beam focused ion beam (FIB). The milling was done at a 52° tilt angle with a 30-kV gallium (Ga) ion beam operating at a current of 30 pA. Initial trench milling of the sample was done at 20 nA and the final face milling at 1 nA to 3 nA. Extra FIB images were taken with the Ga ion beam at a current of 11 pA. The metal composition for each sample was determined with an SEM using energy-dispersive spectroscopy (EDS). All measurements were performed with an accelerating voltage of 15 kV, a probe current of 1150 pA, and a 30-s acquisition time. Lastly, all samples were analyzed with x-ray diffraction (XRD) equipment set at Cu Kα radiation (λ = ~1.54 Å) and Bragg angle (θ) of 136°. The square map function was used to acquire 16 different stress measurements per sample in order to calculate the average stress value accurately for each case; −40° to 40° was the range of ψ angles. The reported results represent an average of multiple independent inspections of the plated surface finishes for each case, with an average of four coupons per case.

RESULTS AND DISCUSSION

Analysis of the Topography and Microstructure of the Sn-Alloy Coatings

Among the various factors that contribute to growth of Sn whiskers, the orientation of the grain boundaries, which serve as major diffusion paths for elements, enhances the process of whisker formation in pure Sn.[2,9] As reported, the columnar grain structure inherent to pure Sn allows uneven diffusion of elements and development of compressive stresses in the Sn film, which lead to growth of Sn whiskers.[9–11] When a Sn coating is applied on a Cu-based substrate, a fast chemical reaction occurs between Cu and Sn, forming Cu_6Sn_5 IMCs, which increase in volume over time and also increase compressive stresses in the film.[9–11]

In an effort to modify the columnar grain structure of pure Sn and analyze its effect on Sn whisker growth, pulse plating deposition of Sn-Bi, Sn-Cu, and Sn-Zn alloy coatings onto a brass substrate were studied. The deposition of the three Sn-alloy coatings by pulse plating technique modified the top surface structure and the microstructure of pure Sn.

Figure 1 presents the topography of each of the three alloy cases, including pure Sn, within 1 day of plating. Based on Fig. 1a and b, the application of a Sn-Bi alloy coating (Fig. 1b) by the pulse plating method produced grains smaller in diameter (approximately 2 μm) than those from the pure Sn surface (approximately 4 μm, Fig. 1a). On the other hand, the alloy coating with Sn-Cu showed a slight increase in surface roughness (Fig. 1c) compared with pure Sn, possibly resulting from the deposition by pulsed current with a shorter off cycle of 5 s (Table I). As reported, shorter off cycles could increase grain deposition onto the substrate and in turn increase surface roughness.[4] Drastic changes in the surface topography and the grain size of the Sn-Zn alloy coating were not noticed (Fig. 1d). However, Zn tends to oxide very quickly in the environment. Thus, significant amounts of zinc precipitates were noticed on the Sn-Zn alloy surface (Fig. 1d). Additionally, the Sn-Zn alloy coating case was the only case that showed significant corrosion on the surface within only 1 week of plating. None of the other cases had any corrosion in the test period of 6 months.

One advantage of Sn-Pb alloy coating in mitigation of Sn whisker growth is the ability of Pb to naturally modify the columnar grain structure of Sn into an equiaxed grain structure.[6,12–14] The equiaxed grain structure of the Sn-Pb alloy can mitigate the formation of Sn whiskers by allowing any compressive stress (considered the driving force for Sn whisker growth), caused by the migration of Cu atoms into the Sn film and the self-diffusion of Sn, to be relieved in the lateral direction rather than to be constrained by vertical, columnar grain boundaries.[6,15]

Natural modification of the columnar grain structure of pure Sn into an equiaxed grain structure is not possible with any alloying element but Pb, unless the plating conditions are modified as they were in this study. As a result, using a pulse plating method for deposition of all three Sn alloy coatings (Sn-Bi, Sn-Cu, and Sn-Zn) resulted in favorable disruption of the columnar grain structure of pure Sn into the desired equiaxed grain structure in each case. Within 1 day of plating, FIB cutting was performed for each case in this study. The results are presented in Fig. 2. Figure 2a shows clear formation of the columnar grain structure in pure Sn. The application of a Sn-Bi alloy coating resulted in a very fine equiaxed grain structure as expected (Fig. 2b).

At room temperature, Sn is well above the temperature required for bulk recrystallization to occur.[1] Freshly plated parts with Sn or Sn alloys begin immediate recrystallization upon removal from the plating bath.[1] Cu in contact with freshly plated Sn films rapidly diffuses into Sn grain boundaries, forming Cu_6Sn_5 IMCs.[1,11] Similarly, in this report, the case with the Sn-Cu alloy coating formed an equiaxed arrangement of grains but,
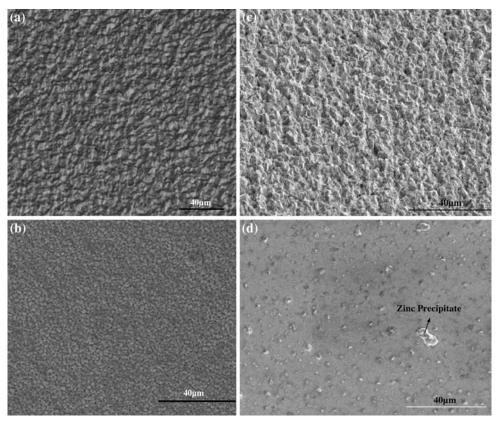
Fig. 1. SEM images of the topography of the plated surface for (a) pure Sn, (b) Sn-Bi alloy, (c) Sn-Cu alloy, and (d) Sn-Zn alloy plating, within 1 day of plating.
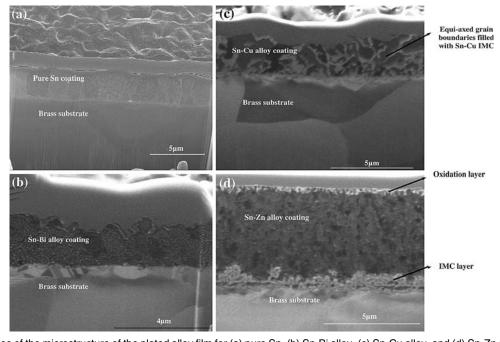

Fig. 2. SEM images of the microstructure of the plated alloy film for (a) pure Sn, (b) Sn-Bi alloy, (c) Sn-Cu alloy, and (d) Sn-Zn alloy plating, within 1 day of plating.

due to the fast reaction of Cu and Sn, formation of Cu_6Sn_5 IMCs almost entirely populated the grain boundaries of the plated film (Fig. 2c). The Cu_6Sn_5 intermetallics, in turn, can induce compressive stresses in the film, but the effect on Sn whisker growth also depends on whether the film has a

columnar or equiaxed grain structure, as with the case of Sn-alloy coatings.

The case with the Sn-Zn alloy coating developed a slightly different equiaxed grain structure compared with the cases of Sn-Bi and Sn-Cu alloy films (Fig. 2d). Formation of a nonuniform IMC layer was noticed right at the coating/substrate interface and the oxidation layer developed on the top surface of the plated film. The oxidation layer formed at the surface of the Sn-Zn alloy coating may have accelerated the growth of Sn whiskers in this case.[16]

Effect of Sn-Alloy Coatings on Mitigation of Sn Whisker Growth After 6 Months of Environmental Exposure

Application of Sn alloy coatings on a brass substrate by the pulse plating method resulted in an equiaxed grain structure for each case. In order to evaluate the effects of the equiaxed microstructure for each alloy coating on the growth of Sn whiskers, we exposed all three cases, including the case with a pure Sn coating, to three environmental conditions of room temperature, elevated temperature of 60°C, and 95% humidity (for details, see the "Experimental Procedures" section) over a period of 6 months. The pure Sn coating initially grew hillocks within the first month at room temperature. As time progressed, the hillocks formed on the pure Sn film,

were influenced by the more extreme environment, such as elevated temperature (60°C) and 95% humidity, and continued to grow into whiskers with an average length of up to 20 μm over the 6-month period, populating the entire plated surface (Fig. 3a).

The case with the Sn-Bi alloy coating did not show any signs of hillock or whisker growth during exposure to room temperature or to 95% humidity. The first signs of hillocks formed on the Sn-Bi alloy film were detected only on the samples exposed to an elevated temperature of 60°C at the sixth month of exposure of the plated samples with Sn-Bi alloy (Fig. 3b). A Sn-Bi alloy coating can drastically increase the incubation period of Sn whisker growth compared with a pure Sn coating under extreme environmental conditions. The magnification in Fig. 3b for the case with the Sn-Bi alloy was increased in order to demonstrate clearly the growth of a few small hillocks detected on the surface. In order to investigate the positive effect of the Sn-Bi alloy coating on the mitigation of Sn whisker growth, a cross-section of the hillock was prepared by FIB. From the cross-section in Fig. 4a, in addition to the equiaxed grain structure, a uniform IMC layer at the coating/substrate interface is noticed, demonstrating very similar behavior to that of a Sn-Pb alloy coating, which can serve as a barrier to the migration of Cu into the Sn-alloy film. Such behavior can
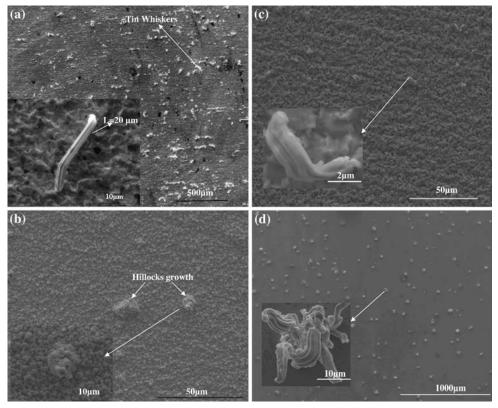

Fig. 3. SEM images of the topography of the plated surface with (a) pure Sn, (b) Sn-Bi alloy, (c) Sn-Cu alloy, and (d) Sn-Zn alloy plating, after 6 months.
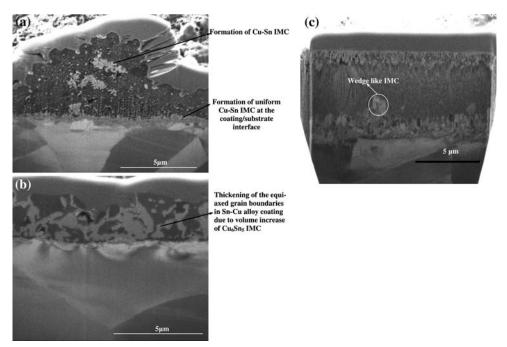
Fig. 4. Microstructure of the plated alloy film for each case: cross-section with (a) Sn-Bi alloy, (b) Sn-Cu alloy, and (c) Sn-Zn alloy plating, after 6 months.

increase the incubation period for growth of Sn whiskers.[12–14] However, despite the many benefits of the Sn-Bi alloy coating, Cu_6Sn_5 IMCs formed in the Sn-Bi alloy film (Fig. 4a) with an elemental composition of Cu (40.46%), Sn (36.89%), Bi (16.03%), and Zn (6.62%). The formation of the Sn-Cu compounds could explain the growth of hillocks on the surface of the Sn-Bi alloy film when exposed to elevated temperature.

The case with the Sn-Cu alloy coating showed signs of whisker growth initially detected under the humid environment after the second month of the study. As time progressed and samples were also exposed to elevated temperature conditions of 60°C, the whiskers grew to an average length of 2 μm to 4 μm during the 6-month test period (Fig. 3c). Approximately 10 to 20 whiskers, 2 μm to 4 μm in length, were detected on the Sn-Cu alloy film after 6 months. The number and length of the whiskers grown from the Sn-Cu alloy film were small; those grown on the alloy film were about ten times shorter than those grown from the pure Sn plated finish over the same time period (Fig. 3a and c). After 6 months under the various environmental influences, an FIB cut was prepared in order to analyze the microstructure of the Sn-Cu alloy film. Thickening of the equiaxed grain boundaries due to increase in volume of the Cu-Sn IMCs was noticed in the microstructure of the alloy film (Fig. 4b). The growth in volume of Cu_6Sn_5 IMCs over time can also affect the stress in the film, and the stress data are presented in detail in the residual stress section of this study. The retarding effect of the Sn-Cu film on the growth of Sn whisker differs from the previously

reported literature. We believe that the ability of the Sn-Cu alloy film to increase the incubation period of Sn whisker growth more than a pure Sn film is due to the presence of the equiaxed microstructure in the Sn-Cu alloy deposit. As reported, if the compressive stresses in the deposit relax by Coble creep, in the case of an equiaxed grain structure in the film, the surface swelling (due to the transport of grains along the grain boundaries) of the film is more uniform, and no localized surface disturbance takes place.[6,14] Additionally, other reports on Sn-Pb alloy coatings present the relationship between IMCs formed in different Sn-based films and claim that Cu_6Sn_5 IMCs form at essentially similar level in pure Sn as in Sn-Pb alloy films.[13,14] Therefore, the different microstructure of pure Sn and Sn-Pb alloy is considered to have an important effect on the mitigation of Sn whisker growth, which is also the main emphasis in this study.

The case with the Sn-Zn alloy coating was drastically affected by corrosion, and some hillocks were noticed on the surface within 2 months of exposure to room temperature. Additionally, the extreme environmental conditions (60°C elevated temperature and 95% humidity) did not influence just the growth of hillocks, but also their population on the surface, which drastically increased compared with the period when the samples were exposed only to room temperature (Fig. 3d). The whiskers in the case of the Sn-Zn alloy coating displayed a unique morphology, a trait not noticed in any of the previous cases (Fig. 3d) in this study. The inspection of the whisker composition, grown from the Sn-Zn alloy surface, revealed that it has some Zn content

Table II. Amount of Whiskers Formed at Various Environments for Each Case During 6 Months

Case Type	Defects on the Surface at Room Temperature	Defects at 95% Humidity	Whisker Growth at Elevated Temperature (60°C)	Population of Whiskers on the Surface After 6 Months
Pure Sn	50 Hillocks	Increased population of hillocks + 30 whiskers (approx. 10 μm in length)	More hillocks + 50 long extruded whiskers with average length of 20 μm and maximum length of 30 μm	Entire surface
Sn-Bi	None	None	5 Hillocks	5 spots detected
Sn-Cu	None	20 Hillocks	More hillocks + 10 whiskers (approx. 4 μm in length)	Approx. 30% of the surface
Sn-Zn	20 Hillocks + corrosion	Hillocks grown in size + increased population of hillocks	Increased population of Sn-Zn hillocks + growth of whiskers (approx. 10 μm in length)	Approx. 75% of the surface

and not only Sn. Zn, like Sn, has the affinity to develop Zn whiskers on its own.[2,17] Also, the accelerated oxidation behavior of Zn most likely contributed to the increased population of Sn whiskers in the Sn-Zn alloy film, unlike the other Sn-alloy films in this study. The microstructure was also inspected using an FIB cut (Fig. 4c). An interesting phenomenon noticed from the microstructure of the Sn-Zn alloy film was the formation of wedge-like IMCs not present in any of the previous cases reported in this study (Fig. 4c). This unique trait that occurred between Sn, Zn, and Cu in the Sn-Zn alloy film was analyzed in the literature as islands of Cu and Zn regions surrounded by a continuous matrix of Sn.[2,18] Additional studies are needed to fully understand this ability of Zn, Cu, and Sn. Furthermore, EDS composition analysis of the microstructure of the Sn-Zn alloy coating showed that, over time, zinc is not permanently attached to the Sn matrix of the film, but it has the affinity to migrate preferentially toward the surface. Similar conclusions on the behavior of Zn are reported by other studies in the literature.[17,18]

The overall summary of the response of each Sn alloy film, including the pure Sn film, to specific environments is listed in Table II.

Residual Stress Measurements of the Sn-Alloy Finish for Each Case

The reported effect for each alloy coating on the mitigation of Sn whisker growth was also related to the stress distribution over time. While views differ slightly within the research community, it is generally recognized that the asymmetrical diffusion of Cu into the grain boundaries and bulk crystals of the Sn film result in the development of compressive stress.[2] The compressive stress is then the driving force for Sn whisker formation, as first demonstrated by Dr. Tu from UCLA in 1973.[2,16] The Cu species in the Sn film causing the increase of compressive stress was initially attributed to the rapidly formed Cu_6Sn_5 intermetallics, although it was later pointed out that the molar volume of the Cu_6Sn_5 intermetallics is less than that of the diffusing Cu atoms.[19] The presence of either species in the Sn matrix should increase the overall stress, as both are greater in weight than Sn, leading to the conclusion that compressive stresses are the driving force for the formation of Sn whisker growth.[2,20,21]

The average stress distribution for each alloy coating was evaluated during the test period of 6 months using an x-ray diffraction (XRD). An XRD with Cu Kα radiation source was used to evaluate the stresses in the top Sn film for each case. The incident x-ray beam was initially positioned perpendicular to the sample with beta (β) set to 0°. β is the main reference point for two x-ray detectors located at ψ_1 and ψ_2 for each β angle.[22] Figure 5 shows an overview of the XRD angles.[19] Psi (ψ) angles are calculated from the β angle using Eq. 1.

$$\psi = \beta \pm (180° - \theta)/2. \tag{1}$$

For this study, the range for β is from 20° to −20° with 11 divisions in this range. At $\beta = 0°$ for Sn, the Bragg angle (θ) is 136°.[22] In order to obtain average residual stress data, the XRD samples a large number of grains that are randomly oriented in a plane parallel to the surface being measured (Fig. 5). The instrument is rotated during the measurement to sample different orientations of these grains relative to a stress direction of interest. The stresses are measured at the macroscopic level: XRD samples multiple grains with β ranging from 20° to −20°, and the local average residual stress at that location (point) is recorded. Sixteen stress points were recorded per sample. The x-ray penetration depth into the film at each location is constant and approximately 2 μm.

The XRD treats the distance between crystallographic planes, called the *d*-spacing, as a strain gage measure.[22] Thousands of grains are typically
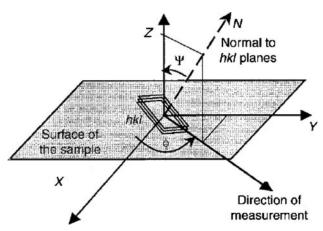
Fig. 5. Direction of stress measurement with XRD.

sampled per measurement. When the material is in tension, the d-spacing increases in the direction of stress, and when the material is in compression, the d-spacing decreases. For a known x-ray wavelength ($\lambda = 1.54$ Å) and number of wavelengths (n) equal to unity, the diffraction angle, 2θ, is measured experimentally, and the d-spacing is then calculated using Bragg's law (2).[22]

$$d = \frac{n\lambda}{2\sin\theta}. \qquad (2)$$

Strain is calculated using Eq. 3, where d_0 is considered the interplanar distance for an unstressed condition of the material at $\psi = 0°$.

$$\varepsilon = \frac{d - d_0}{d_0}. \qquad (3)$$

XRDWin software (version 2.0) was used to calculate the average residual stress values based on Hooke's law, from the strain distributions.[22–24] The elastic modulus and Poisson ratio of Sn, E, and v, are set to 42 GPa and 0.36 GPa, respectively.[1]

The average stress results over 6 months under environmental exposure are presented in Fig. 6 for all three alloy coatings, including the case of a pure Sn plating. The average stresses for each case were calculated every couple of weeks over 6 months by collecting 16 independent stress measurements per case using a square map function. The measurements were taken over an area of 1 cm^2 at the center of the surface of each coupon. The XRD measures the stresses in the plated film for each case. The stresses for each case were measured at the same location where samples were inspected for whiskers in the earlier sections of this study. Based on the stress distribution in Fig. 6, the pure Sn coating displayed an average compressive stress of -29 MPa and maximum compressive stress of -48 MPa (Fig. 6a). The Sn-Bi alloy showed the lowest average compressive stress distribution of approximately -10 MPa, as well as the lowest maximum compressive stress of -20 MPa of all the
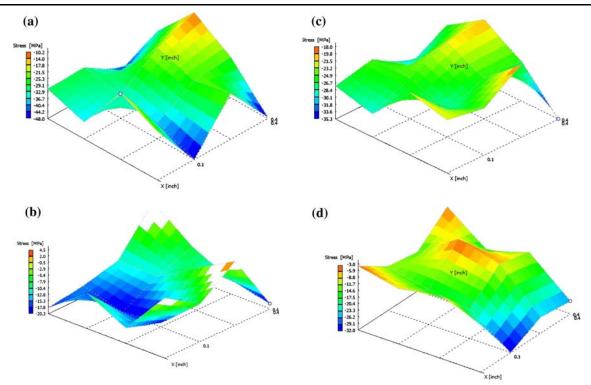

Fig. 6. XRD images of the stress distribution over the 6-month test period for (a) pure Sn, (b) Sn-Bi alloy, (c) Sn-Cu alloy, and (d) Sn-Zn alloy film.

cases studied (Fig. 6b). The lowest compressive stress formed in the Sn-Bi alloy film possibly contributed to the increased incubation period for Sn whisker growth reported previously for this case. Some locations inside the Sn-Bi alloy film had a tensile stress of 0 MPa to 4.5 MPa (Fig. 6b), which most likely balanced the compressive stress of the film and resulted in a lower stress distribution compared with the other cases studied. The Sn-Cu alloy film resulted in a slightly lower average and maximum compressive stress of −26 MPa and −35 MPa, respectively, compared with the pure Sn film (Fig. 6c). The Sn-Zn alloy coating developed an average compressive stress of −17 MPa and maximum stress of −29 MPa, which was lower than that of the pure Sn plating, but also slightly lower than the stress of the Sn-Cu alloy film.

CONCLUSION

The effects of three pulsed electrodeposited Sn alloy films on a Cu-based substrate were investigated under different environmental conditions and over particular time periods. Modified grain structure using a pulsed plating technique was achieved with Sn-Bi, Sn-Cu, and Sn-Zn alloy films. All three studied Sn alloy films increased the incubation period of Sn whisker growth compared with a pure Sn plating. Similarly, the formation of the equiaxed grain structure can be the main reason that the deposited Sn-Cu alloy film was able to increase the incubation period of Sn whisker growth compared with the pure Sn film. Sn-Zn and Sn-Cu alloy films are thus good candidates to modify the microstructure of a pure Sn coating, but they are not adequate elements for the mitigation of Sn whisker growth over a longer time period. Despite the ability of the Sn alloys to modify the columnar microstructure inherent to pure Sn, whiskers still grew from the electroplated surfaces, indicating that the arrangement of the grain structure in the Sn-based film was an important but not the sole factor that contributes to the growth of Sn whiskers. Other factors, such as the amount of Cu migration into the film and the formation of Sn-Cu IMCs, could hinder the ability of the alloy film to impede the growth of Sn whiskers.

The case with a Sn-Bi alloy coating could display better results if a nickel (Ni) underlayer was applied prior to the Sn-Bi finish. The Ni underlayer could prevent the migration of Cu into the Sn alloy film and decrease the formation of the localized build-up of Cu-Sn IMCs, which can reduce Sn whisker growth over a longer time period than that presented in this study. However, additional studies are needed to confirm the efficiency of a Sn-Bi alloy coating with a Ni underlayer. Additionally, this study was also performed with indium (In) and Ni

as alloying elements with Sn. However, our experiments proved that these two elements (In and Ni) require additional process modifications for concentration weighting and increased current density in order to form alloy depositions (Sn-In and Sn-Ni) with Sn.

REFERENCES

1. J.W. Price, *Tin and Tin Alloy Plating* (Ayr, Scotland: Electrochemical, 1983).
2. G.T. Galyon, *IEEE Trans. Electron. Packag. Manuf.* 28, 94 (2005).
3. S.M. Arnold, *Plating* 53, 96 (1966).
4. J.C. Puippe and F. Leaman, *Theory and Practice of Pulse Plating* (Orlando, FL: AES, 1986).
5. M. Chen, S. Ding, Q. Sun, D.W. Zhang, and L. Wang, *J. Electron. Mater.* 37, 894 (2008).
6. E. Sandnes, M.E. Williams, M.D. Vaudin, and G.R. Stafford, *J. Electron. Mater.* 37, 490 (2007).
7. [Online] Available at http://www.jesuitnola.org/upload/clark/refs/red_pot.htm (2009).
8. M.P. Groover, *Fundamentals of Modern Manufacturing*, 3rd ed. (Hoboken, NJ: Wiley, 2007), p. 3e.
9. C. Xu, Y. Zhang, C. Fan, J. Abys, L. Hopkins, and F. Stevie. *Proceedings of the IPC SMEMA APEX Conference*, S-06-2-1 (2002).
10. K. Whitlaw and J. Crosby. *Proceedings of the AESF SUR/FIN Conference* (2002), p. 19.
11. M.-H. Lu and K.-C. Hsieh, *J. Electron. Mater.* 36, 1448 (2007).
12. W. Zhang and F. Schwager, *J. Electrochem. Soc.* 153, C337 (2006).
13. E. Chason, N. Jadhav, W.L. Chan, L. Reinbold, and K.S. Kumar. *Appl. Phys. Lett.* 92, 171901 (2008).
14. W.J. Boettinger, C.E. Johnson, L.A. Bendersky, K.W. Moon, M.E. Williams, and G.R. Stafford, *Acta Mater.* 53, 5033 (2005).
15. R. Schetty, *Proceedings of the IPC Works*, S-02-3-1 (2000).
16. K.N. Tu, *Acta Metall.* 21, 347 (1973).
17. K.J. Puttlitz and K.A. Stalter, *Handbook of Lead-Free Solder Technology for Microelectronic Assemblies* (New York: Marcel Dekker, 2004).
18. S.C. Britton and M. Clarke, *Proceedings of the 6th International Metal Finishing Conference* (1964), p. 205.
19. B.Z. Lee and D.N. Lee, *Acta Mater.* 46, 3701 (1998).
20. J. Smetana, *J. IEEE Trans. Electron. Packag. Manuf.* 30, 1 (2007).
21. iNEMI Recommendations on Lead-Free Finishes for Components Used in High-Reliability Products, Version 4 (2006).
22. J.A. Pineault, M. Belassel, and M.E. Brauss, *X-Ray Diffraction Residual Stress Measurement in Failure Analysis* (Old Castle, Canada: Proto Manufacturing Ltd., 2009).
23. P.J. Withers and H.K.D.H. Bhadeshia, *Mater. Sci. Technol.* 17, 355 (2001).
24. A.D. Krawitz, R.A. Winholtz, and C.M. Weisbrook, *Mater. Sci. Eng.* A206, 176 (1995).